Title

RADIONUCLIDE MIGRATION THROUGH FRACTURED ROCK: EFFECTS OF MULTIPLE FRACTURES AND TWO-MEMBER DECAY CHAINS

Authors

Ann, J.
Chambre, P.L.
Pigford, T.H.

Publication Date

1985-09-01

LBL-21121
UC-70

Lawrence Berkeley Laboratory
UNIVERSITY OF CALIFORNIA

EARTH SCIENCES DIVISION

Radionuclide Migration through Fractured Rock: Effects of Multiple Fractures and Two-Member Decay Chains

J. Ahn, P.L. Chambré, and T.H. Pigford

September 1985

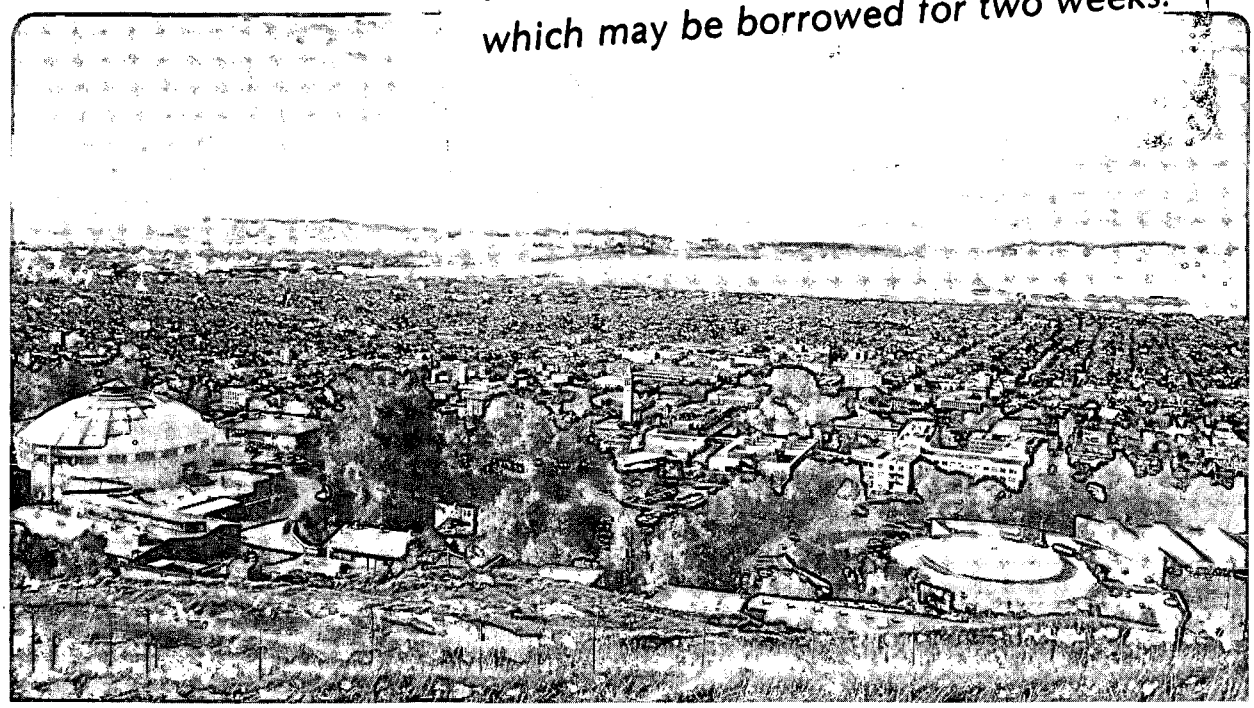

Prepared for the U.S. Department of Energy under Contract DE-AC03-76SF00098

DISCLAIMER

LBL-21121

RADIONUCLIDE MIGRATION THROUGH FRACTURED ROCK: EFFECTS OF MULTIPLE FRACTURES AND TWO-MEMBER DECAY CHAINS

J. Ahn, P. L. Chambré, and T. H. Pigford

Earth Sciences Division, Lawrence Berkeley Laboratory

and

Department of Nuclear Engineering

University of California

Berkeley, CA 94720

Manuscript completed September 1985

Work supported in part by U. S. Department of Energy contract DE-AC03-76SF00098

The authors invite comments and would appreciate being notified of any errors in the report.

T. H. Pigford
Department of Nuclear Engineering
University of California
Berkeley, CA 94720

ACKNOWLEDGEMENT

This research was supported in part by the U. S. Department of Energy, Office of Civilian Radioactive Waste Management, Repository Technology Program. The conclusions of the authors are not necessarily endorsed or approved by the U. S. Department of Energy.

REPORT OUTLINE

RADIONUCLIDE MIGRATION THROUGH FRACTURED ROCK: EFFECTS OF MULTIPLE FRACTURES AND TWO-MEMBER DECAY CHAINS

1. Introduction and Summary

This report presents the results of an analytical study of the hydrological transport of a radioactive contaminant through fractured, porous rock. The purpose is to evaluate the time-, and space-dependent concentration of the contaminant in the ground-water in the fractures and in the rock pores.

In a previous report[1] we presented analytical solutions for transport of a sorbing radionuclide with no decay precursors through a single fracture, with and without dispersion. The importance of matrix diffusion was shown. Diffusion from the fracture into the rock matrix retards contaminant transport through the fracture even without sorption in the medium. In the present report we extend the previous work in two directions: multiple parallel fractures and a two-member decay chain. In some instances the contaminant penetrates so deeply into the rock matrix that concentration fields from adjacent fractures overlap, requiring consideration of multiple fractures in predicting contaminant transport. Migrating decay presursors can affect the concentration field of their daughters because the daughters are generated inside the rock and the fracture as well as in the repository.

Sudicky and Frind[3,4] also gave analytical solutions for these problems, but their solutions for a system of multiple parallel fractures[3] contain several apparently incorrect expressions. Their analytical solution for the concentration in the fractures does not satisfy the boundary condition at the fracture entrance. And their analytical solution for the concentration in a porous matrix does not satisfy the boundary condition at the rock/fracture interface, either.

We provide corrected version of the Sudicky and Frind solutions, and we propose a simplified analytical method that superposes two single-fracture solutions for the concentration in the rock matrix with a system of parallel fractures. The exact solutions require multiple integrals and summation of an infinite series, which converges slowly because of its oscillating nature. The convergence of the series becomes slower for strongly-

sorbing media, large spacing of two fractures, and early times. The superposition is valid, on the other hand, for these three cases. We show the validity of the approximation in terms of the Fourier modulus and (t, R_p) space, where t is time and R_p the pore retardation coefficient. Validity is also a function of the assumed release mode. The approximation is valid for a larger domain for the step release than for the band release mode in (t, R_p) space.

Since the Sudicky and Frind's solutions for a two-member decay chain are obtained for an impulse release at the repository boundary, we can use them as Green's functions in convolution integrals to obtain solutions for arbitrary release modes. We calculate, for example, the concentrations for the exponentially decaying step release by making the convolution of their solutions and the step function. We compare these results with our previous numerical results[6] approximated by neglecting decay in the rock matrix, and find that this approximation introduces considerable errors especially in the case of the daughter nuclide at far field from the repository.

In summary, we made extension to the theory of radionuclide penetration into multiply fractured rock, and provided solutions for a two-member decay chain.

2. Evaluation of the Sudicky and Frind's Solutions

In a series of papers, Tang, Sudicky and Frind[2,3,4] presented solutions for contaminant transport in multiple rock fractures. The system they considered is shown in Figure 2.1. We first present a review and evaluation of their work.

2.1 Analytical solutions for a System of Parallel Fractures

Tang, Sudicky and Frind showed analytical solutions for contaminant transport through equally-spaced, parallel fractures by advection and dispersion, and diffusion into the rock matrix. Sorption retardation of the movement of the contaminant in both fractures and rock pores is considered. Radioactive decay is considered without any precursors. Each fracture is identical. The governing equations are:

$$\frac{\partial N}{\partial t} + \frac{v}{R_f}\cdot\frac{\partial N}{\partial z} - \frac{D}{R_f}\cdot\frac{\partial^2 N}{\partial z^2} + \lambda N + \frac{q}{bR_f} = 0, \qquad 0 < z < \infty, \tag{2.1}$$

$$\frac{\partial M}{\partial t} - \frac{D_p}{R_p}\cdot\frac{\partial^2 M}{\partial y^2} + \lambda M = 0, \qquad b < y < 2S - b, \tag{2.2}$$

where

$N(z,t)$	:	concentration in the water in fractures, kg/m^3,
$M(y,z,t)$	:	concentration in rock pores, kg/m^3,
v	:	groundwater velocity, m/yr,
D	:	dispersion coefficient in fractures, kg/m^2·yr,
D_p	:	diffusion coefficient in rock pores, kg/m^3·yr,
λ	:	decay constant, yr $^{-1}$,
b	:	half width of fractures, m,
S	:	half spacing of fractures, m.

R_f and R_p are the retardation coefficient defined as

$$R_f = 1 + \frac{K_f}{b} \tag{2.3}$$

$$R_p = 1 + \frac{a_p}{\varepsilon}\cdot K_p \tag{2.4}$$

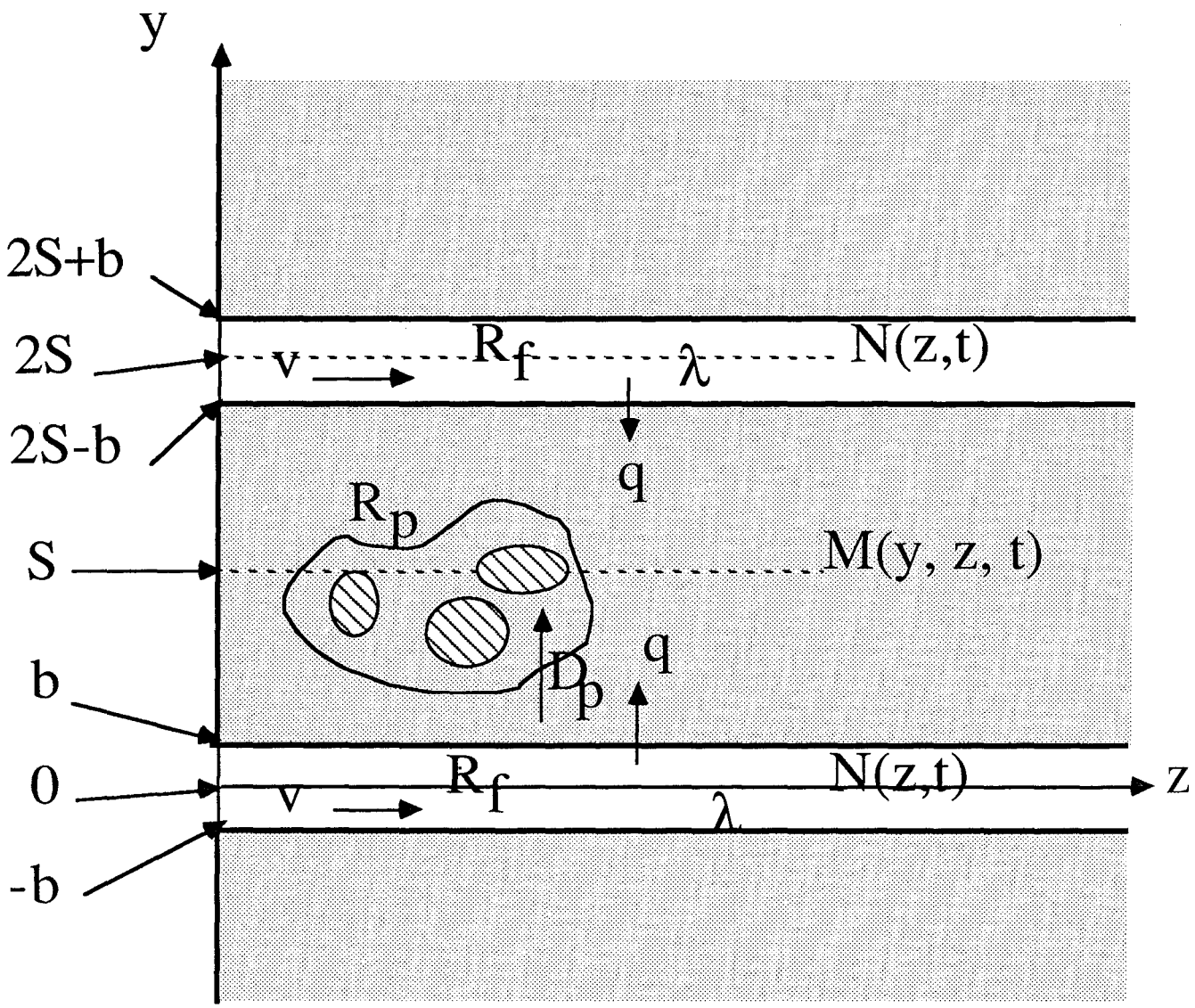

Fig. 2.1 Parallel fractures and porous rock. The system is symmetric with respect to y = S plane because each fracture is identical.

where K_f and K_p are the distribution coefficients for fracture and the pore surfaces ([kg/m²]/[kg/m³]), respectively. a_p is the pore surface area per unit volume of rock matrix (m²-pore surface/m³-rock volume). ε is porosity of rock excluding the pores which are not connected to the fractures. Rock penetration is represented by q in (2.1), the rate of diffusion from a fracture into pores, per unit area of fracture surface (kg/m²yr), and is defined as:

$$q(z, t) = - \varepsilon D_p \cdot \left.\frac{\partial M}{\partial y}\right|_{y=b} , \qquad z > 0, \quad t > 0. \tag{2. 5}$$

If the dispersion coefficient is zero, (2.1) becomes a first-order equation, which may be treated as a special case.

The side conditions are:

$$N(z,0) = 0, \qquad z > 0, \tag{2.6a}$$

$$M(y,z,0) = 0, \qquad b < y < S, z > 0, \tag{2.6b}$$

$$N(0,t) = \psi(t), \qquad t > 0, \tag{2.6c}$$

$$N(\infty,t) = 0, \qquad t > 0, \tag{2.6d}$$

$$M(b,z,t) = N(z,t) \qquad z > 0, t > 0, \tag{2.6e}$$

$$\left.\frac{\partial M}{\partial y}\right|_{y=S} = 0, \qquad z > 0, t > 0, \tag{2.6f}$$

(2.6f) is the difference from the single-fracture problem[1]. In our previous analysis, an infinite amount of rock was assumed to surround a fracture. Side condition (2.6f) limits the amount of rock surrounding each fracture. $\psi(t)$ represents the release characteristics at the repository. Sudicky and Frind have applied the step release:

$$\psi(t) = N^\circ h(t), \tag{2.7}$$

where N° is the concentration at the repository. They have made use of Laplace transforms and obtained the following solutions. However, these solutions contain apparently incorrect expressions. We show below the corrected version and note the corrected parts with boxes.

For non-zero D:

$$\frac{N}{N^\circ}=\frac{2}{\pi^{3/2}}e^{vz}\int_g^\infty e^{-\xi^2-\frac{v^2z^2}{4\xi^2}-\lambda YA}\int_0^\infty\frac{\mu\cdot e^{\mu_R}}{\lambda^2+\frac{\mu^4}{4}}\cdot\left[e^{-\lambda T}\left\{\frac{\mu^2}{2}\cdot\sin(\mu_g|_T)-\lambda\cos(\mu_g|_T)\right\}+\frac{\mu^2}{2}\sin(\Omega)+\lambda\cos(\Omega)\right]d\mu d\xi$$

$z\geq 0,\ t\geq 0,$ (2.8)

$$\frac{M}{N^\circ}=\frac{2}{\sqrt{\pi}\,\sigma^2}\sum_{n=0}^\infty(-1)^n(2n+1)\cos\left[\frac{(2n+1)\pi(S-y)}{2(S-b)}\right]e^{vz}\int_g^\infty e^{-\xi^2-\frac{v^2z^2}{4\xi^2}-YA}\int_0^\infty\frac{\mu\cdot e^{\mu_R}}{\lambda^2+\frac{\mu^4}{4}}\cdot\left[\frac{e^{-\lambda T}}{\omega^2+\frac{\mu^4}{4}}\left\{\frac{\mu^2}{2}\{\omega\cdot\sin(\mu_g|_T)\right.\right.$$

$$-\frac{\mu^2}{2}\cdot\cos(\mu_g|_T)\}-\lambda\{\omega\cdot\cos(\mu_g|_T)+\frac{\mu^2}{2}\sin(\mu_g|_T)\}+e^{-\omega T}\left\{\frac{\mu^2}{2}\omega\boxed{\sin(\Omega)}+\frac{\mu^4}{4}\boxed{\cos(\Omega)}+\lambda\omega\boxed{\cos(\Omega)}\right.$$

$$\left.\left.-\frac{\lambda\mu^2}{2}\boxed{\sin(\Omega)}\right\}\right\}+\frac{1}{\boxed{\omega+\lambda}}[1-\boxed{e^{-(\omega+\lambda)T}}]\cdot\left\{\frac{\mu^2}{2}\sin(\Omega)+\lambda\cdot\cos(\Omega)\right\}\Bigg]d\mu d\xi,$$

$b<y<2S-y,\ z>0,\ t\geq 0.$ (2.9)

For D = 0:

$$\frac{N}{N^\circ}=\frac{1}{\pi}\boxed{e^{-\lambda ZA}}h(t-ZA)\int_0^\infty\frac{\mu\cdot e^{\mu_R^\circ}}{\lambda^2+\frac{\mu^4}{4}}\left[e^{-\lambda T^\circ}\left\{\frac{\mu^2}{2}\sin(\mu_g^\circ|_{T^\circ})-\lambda\cdot\cos(\mu_g^\circ|_{T^\circ})\right\}+\frac{\mu^2}{2}\sin(\Omega^\circ)+\lambda\cdot\cos(\Omega^\circ)\right]d\mu,$$

$z\geq 0,\ t\geq 0,$ (2.10)

$$\frac{M}{N^\circ}=\frac{1}{\sigma^2}\sum_{n=0}^\infty(-1)^n(2n+1)\cdot\cos\left[\frac{(2n+1)\pi(S-y)}{2(S-b)}\right]\boxed{e^{-\lambda ZA}}h(t-ZA)\cdot\int_0^\infty\frac{\mu\cdot e^{\mu_R^\circ}}{\lambda^2+\frac{\mu^4}{4}}\left[\frac{e^{-\lambda T^\circ}}{\omega^2+\frac{\mu^4}{4}}\left\{\frac{\mu^2}{2}\left\{\omega\cdot\sin(\mu_g^\circ|_{T^\circ})\right.\right.\right.$$

$$\left.-\frac{\mu^2}{2}\cdot\cos(\mu_g^\circ|_{T^\circ})\right\}-\lambda\cdot\left\{\omega\cdot\cos(\mu_g^\circ|_{T^\circ})+\frac{\mu^2}{2}\cdot\sin(\mu_g^\circ|_{T^\circ})\right\}+\boxed{e^{-\omega T^\circ}}\left\{\frac{\mu^2}{2}\cdot\omega\cdot\boxed{\sin(\Omega^\circ)}\right.$$

$$\left.\left.+\frac{\mu^4}{4}\cdot\boxed{\cos(\Omega^\circ)}+\lambda\omega\boxed{\cos(\Omega^\circ)}-\frac{\lambda\mu^2}{2}\cdot\boxed{\sin(\Omega^\circ)}\right\}\right\}+\frac{1}{\boxed{\omega+\lambda}}\left[1-\boxed{e^{-(\omega+\lambda)T^\circ}}\right]$$

$$\left\{\frac{\mu^2}{2}\cdot\sin(\Omega^\circ)+\lambda\cdot\cos(\Omega^\circ)\right\}\Bigg]d\mu,\qquad b<y<2S-y,\ z>0,\ t\geq 0,$$ (2.11)

where

$$T = t - YA, \qquad Y = \frac{\nu^2\beta^2 z^2}{4A\xi^2}, \qquad \nu = \frac{v}{2D}, \qquad \beta^2 = \frac{4R_f D}{v^2}$$

$$T^o = t - ZA, \qquad Z = \frac{R_f z}{vA}, \qquad A = \frac{bR_f}{\varepsilon\sqrt{D_p R_p}},$$

$$\mu_R = -\frac{Y}{2}\cdot P_1(\mu), \qquad \mu_g = \frac{\mu^2 t}{2} - \frac{Y}{2}\cdot P_2(\mu), \qquad \Omega = \frac{Y}{2}\cdot P_2(\mu),$$

$$\mu_R^o = -\frac{Z}{2}\cdot P_1(\mu), \qquad \mu_g^o = \frac{\mu^2 t}{2} - \frac{Z}{2}\cdot P_2(\mu), \qquad \Omega^o = \frac{Z}{2}\cdot P_2(\mu),$$

$$P_1(\mu) = \mu\left[\frac{\sinh(\sigma\mu) - \sin(\sigma\mu)}{\cosh(\sigma\mu) + \cos(\sigma\mu)}\right], \qquad P_2(\mu) = \mu\left[\frac{\sinh(\sigma\mu) + \sin(\sigma\mu)}{\cosh(\sigma\mu) + \cos(\sigma\mu)}\right],$$

$$\sigma = B(S - b), \quad B = \sqrt{\frac{R_p}{D_p}}, \quad g = \frac{z}{2}\cdot\sqrt{\frac{R_f}{D\cdot t}}, \quad \omega = \frac{\pi^2(2n+1)^2}{4\sigma^2}. \qquad (2.12)$$

These errors shown in eqs. (2.8) to (2.11) may come from the incorrect time integration. In order to obtain the solution for N/N° they apparently applied the identity:

$$L^{-1}\left[e^{-YAp}\cdot\tilde{f}(p)\right] = h(t - YA)\cdot f(t - YA), \quad YA \geq 0 \qquad (2.13)$$

where p and $L^{-1}[\ ]$ stand for the variable and inverse Laplace transform, respectively. In Sudicky and Frind's solution to N/N° for non-zero D, the Heaviside step function, h(t-YA), has been taken into account by changing the integration with respect to ξ in (2.8) from $\int_0^\infty$ to $\int_g^\infty$, $g = \frac{z}{2}\cdot\sqrt{\frac{R_f}{D\cdot t}}$.

By this manipulation, T = t - YA remains non-negative in the interval, $\xi \geq 1$. For D = 0, h(t-ZA) is included in (2.10). Then they obtained the solution for M/N° by taking the inverse transform of

$$\tilde{M}(y, z, p) = \tilde{N}(z, p)\frac{\cosh\left(B\sqrt{p+\lambda}\,(S-y)\right)}{\cosh\left(B\sqrt{p+\lambda}\,(S-b)\right)}, \qquad (2.14)$$

with the convolution theorem:

$$L^{-1}\left[\tilde{f}_1(p)\cdot\tilde{f}_2(p)\right]=\int_0^t f_1(\tau)f_2(t-\tau)\,d\tau, \tag{2.15}$$

where, in their case,

$$\tilde{f}_1(p)=\tilde{N}\ (z,p),\quad \text{and}\quad f_1(t)=N(z,t) \tag{2.16}$$

$$\tilde{f_2}(p)=\frac{\cosh\left(B\sqrt{p+\lambda}\cdot(S-y)\right)}{\cosh\left(B\sqrt{p+\lambda}\cdot(S-b)\right)},\ \text{and}\ f_2(t)=\frac{\pi}{B^2(S-b)^2}\sum_{n=0}^{\infty}(-1)^n(2n+1)e^{-(\omega+\lambda)t}\cos\left[\frac{(2n+1)\pi(S-y)}{2(S-b)}\right] \tag{2.17}$$

In case of non-zero D, they have made the time integration in (2.15) after substitution of (2.16) and (2.17), ignoring the fact that the lower limit of the integral with respect to ξ in (2.8) becomes a function of τ, i.e., $g(\tau)=\frac{z}{2}\cdot\sqrt{\frac{R_f}{D\tau}}$. In the case of D = 0, they apparently ignored the presence of h(t-ZA) in (2.10) on substitution of (2.10) into (2.15).

Even after these corrections, equations from (2.8) to (2.12) require further consideration.

First, let us consider whether or not eqs. (2.8) and (2.10) satisfy the boundary condition (2.7). Substituting z = 0 into (2.10), for example, yields

$$\frac{N(0,t)}{N^\circ}=\frac{1}{\pi}h(t)\int_0^\infty\frac{\mu}{\lambda^2+\frac{\mu^4}{4}}\left[e^{-\lambda t}\left\{\frac{\mu^2}{2}\cdot\sin\left(\frac{\mu^2 t}{2}\right)-\lambda\cdot\cos\left(\frac{\mu^2 t}{2}\right)\right\}+\lambda\right]d\mu,$$

which cannot be reduced to h(t). This error arose when the order of two integrations was interchanged: As a result of the inversion of Laplace-transformed solutions, Sudicky and Frind obtained solutions of the following forms:

For non-zero D:

$$\frac{N}{N^\circ}=\frac{2}{\sqrt{\pi^3}}\cdot e^{vz}\int_g^\infty e^{-\xi^2-\frac{v^2z^2}{4\xi^2}-\lambda YA\,T}\int_0^\infty e^{-\lambda\tau}\int_0^\infty\mu\cdot e^{\mu_R}\cos(\mu_g I_\tau)\,d\mu\,d\tau\,d\xi, \tag{2.8'}$$

For D = 0:

$$\frac{N}{N^\circ} = \frac{1}{\pi} \cdot e^{-\lambda ZA} h(t - ZA) \int_0^{T^\circ} e^{-\lambda\tau} \int_0^{\infty} \mu \cdot e^{\mu_R^\circ} \cos(\mu_{g\,\tau}^\circ) d\mu d\tau. \qquad (2.10')$$

They exchanged the order of the integration of μ and τ in the above equations, resulting in eqs. (2.8) and (2.10), respectively. However, this operation is valid only if the following conditions are met[9] (We write the conditions for (2.8'); equivalent ones can be written for (2.10')):

(1) $\exp(-\lambda\tau)\cdot\cos(\mu_{g\,\tau})$ is continuous and bounded for τ and μ on the intervals C: $0 \le \tau \le T$ and Γ: $0 \le \mu < \infty$.

(2) the integral

$$\int_0^{\infty} \mu \cdot e^{\mu_R} d\mu$$

must converge absolutely.

The second condition cannot be met if z = 0 because with z = 0, we have $\mu_R = 0$, and the integral does not converge at all. Hence, (2.8) is not valid for z = 0. By the same reason, (2.10) is not valid for z = 0, either. Thus we must still use (2.8') and (2.10') to satisfy the boundary condition (2.7). To check if (2.8') and (2.10') actually satisfy (2.7), let us substitute z = 0 into (2.8'), for example, obtaining

$$\frac{N(0,t)}{N^\circ} = \frac{2}{\sqrt{\pi^3}} \int_0^{\infty} e^{-\xi^2} \int_0^{t} e^{-\lambda\tau} \int_0^{\infty} \mu \cdot \cos\left[\frac{\mu^2\tau}{2}\right] d\mu d\tau d\xi$$

Considering the identities

$$\frac{2}{\sqrt{\pi}} \int_0^{\infty} e^{-\xi^2} d\xi = 1, \qquad \text{and}$$

$$\int_0^{\infty} \frac{\mu}{\pi} \cdot \cos\left[\frac{\mu^2\tau}{2}\right] d\mu = \int_0^{\infty} \frac{\cos(x\tau)}{\pi} dx = \left[\frac{\sin(x\tau)}{\pi\tau}\right]_0^{\infty} = \lim_{x \to \infty} \frac{\sin(x\tau)}{\pi\tau} = \delta(\tau)$$

where $\delta(\tau)$ is Dirac's delta function, we can obtain the identical form to the boundary condition (2.7) as follows:

$$\frac{N(0,t)}{N^\circ} = \int_0^t e^{-\lambda\tau}\cdot\delta(\tau)d\tau = 1, \quad \text{for } t > 0.$$

By setting y = b, (2.9) and (2.11) should give the same forms as (2.8) and (2.10), respectively, by the boundary condition (2.6e). But they do not. This is because the inverse transform of (2.17) is valid only in the region $b < y < 2S-b$[7] . Hence (2.9) and (2.11) are correct only in this region. In order to avoid this difficulty, we write the Laplace-transformed solution for M/N° explicitly by substituting the Laplace-transformed solution for N/N° into (2.14):

$$\tilde{M}(y,z,p) = N^\circ e^{vz}\; e^{-vz\sqrt{1+\beta^2\left[\frac{1}{A}\sqrt{p+\lambda}\tanh\left(\sigma\sqrt{p+\lambda}\right)+(p+\lambda)\right]}}\;\frac{\cosh\left(B\sqrt{p+\lambda}\cdot(S-y)\right)}{p\cdot\cosh\left(B\sqrt{p+\lambda}\cdot(S-b)\right)} \tag{2.18}$$

Then we take $\tilde{f_1}(p)$ and $\tilde{f_2}(p)$ in (2.15), instead of (2.16) and (2.17), as follows:

$$\tilde{f_1}(p) = \frac{\cosh\left(B\sqrt{p+\lambda}\cdot(S-y)\right)}{p\cdot\cosh\left(B\sqrt{p+\lambda}\cdot(S-b)\right)}, \text{ and} \tag{2.19}$$

$$\tilde{f}_2(p) = N^\circ e^{vz} e^{-vz\sqrt{1+\beta^2\left[\frac{1}{A}\sqrt{p+\lambda}\tanh\left(\sigma\sqrt{p+\lambda}\right)+(p+\lambda)\right]}}, \text{ for non-zero D,} \tag{2.20a}$$

$$\tilde{f}_2(p) = N^\circ\cdot e^{-\frac{R_f z}{v}\left((p+\lambda)+\frac{\sqrt{p+\lambda}}{A}\tanh\left[\sigma\sqrt{p+\lambda}\right]\right)} \quad \text{for } D = 0, \tag{2.20b}$$

and apply the convolution theorem. Then the correct solutions that are valid for $b \le y \le 2S-b$ are:

(i) non-zero D:

$$\frac{M}{N^\circ}=\frac{2}{\pi^{3/2}}\cdot e^{vz-\lambda t}\int_g^\infty e^{-\xi^2-\frac{v^2z^2}{4\xi^2}}\int_0^\infty \mu\cdot e^{\mu_R}\left\{\frac{\cosh\left(B\sqrt{\lambda}\cdot(S-y)\right)}{\left(\lambda^2+\frac{\mu^4}{4}\right)\cosh\left(\sigma\sqrt{\lambda}\right)}\left[\frac{\mu^2}{2}\cdot\sin(\mu_g l_T)-\lambda\cdot\cos(\mu_g l_T)+e^{\lambda T}\left\{\frac{\mu^2}{2}\sin(\Omega)\right.\right.\right.$$

$$\left.\left.\left.+\lambda\cdot\cos(\Omega)\right\}\right]-4\pi\sum_{n=0}^{\infty}\frac{(-1)^n(2n+1)}{(2n+1)^2\pi^2+4\lambda\sigma^2}\cdot\frac{1}{\omega^2+\frac{\mu^4}{4}}\cdot\cos\left[\frac{(2n+1)\pi(S-y)}{2(S-b)}\right]\cdot\left[\frac{\mu^2}{2}\cdot\sin(\mu_g l_T)+\omega\cos(\mu_g l_T)\right.\right.$$

$$\left.\left.+e^{-\omega T}\cdot\left\{\frac{\mu^2}{2}\sin(\Omega)-\omega\cdot\cos(\Omega)\right\}\right]\right\}d\mu d\xi,\quad b\le y\le 2S-b,\quad z>0,\quad t\ge 0, \tag{2.21}$$

(ii) D = 0:

$$\frac{M}{N^\circ}=\frac{1}{\pi}e^{-\lambda ZA}h(t-ZA)\int_0^\infty \mu\cdot e^{\mu_R^\circ}\left\{\frac{\cosh\left(B\sqrt{\lambda}\cdot(S-y)\right)}{\left(\lambda^2+\frac{\mu^4}{4}\right)\cosh\left(\sigma\sqrt{\lambda}\right)}\left[e^{-\lambda T^\circ}\left\{\frac{\mu^2}{2}\cdot\sin(\mu_g^\circ l_{T^\circ})-\lambda\cdot\cos(\mu_g^\circ l_{T^\circ})\right\}\right.\right.$$

$$\left.\left.+\frac{\mu^2}{2}\cdot\sin(\Omega^\circ)+\lambda\cdot\cos(\Omega^\circ)\right]-4\pi\sum_{n=0}^{\infty}\frac{(-1)^n(2n+1)}{(2n+1)^2\pi^2+4\lambda\sigma^2}\cdot\frac{e^{-\lambda T^\circ}}{\omega^2+\frac{\mu^4}{4}}\cdot\cos\left[\frac{(2n+1)\pi(S-y)}{2(S-b)}\right]\cdot\right.$$

$$\left.\left[\frac{\mu^2}{2}\cdot\sin(\mu_g^\circ l_{T^\circ})+\omega\cdot\cos(\mu_g^\circ l_{T^\circ})+e^{-\omega T^\circ}\left(\frac{\mu^2}{2}\sin(\Omega^\circ)-\omega\cdot\cos(\Omega^\circ)\right)\right]\right\}d\mu,\ b\le y\le 2S-b,\ z>0,\ t\ge 0 \tag{2.22}$$

Note that for eqs. (2.21) and (2.22), z = 0 is carefully excluded from their domain of definition because the concentration in the porous rock is considered only in the region $z > 0$, $b \le y \le 2S - b$, $t \ge 0$. Therefore, we can exchange the order of integration with respect to μ and τ in the preceding forms of (2.21) and (2.22), which contain very similar forms to (2.8') and (2.10').

Finally, equations (2.8') and (2.10'), (2.21) and (2.22) are the correct solutions for the concentration in the fractures and for the concentrations in the rock matrix, respectively.

In (2.8'), (2.10'), (2.21) and (2.22), the multiple integrals and the infinite series must be evaluated numerically for the M/N° calculation. In order to achieve reasonable accuracy for numerical evaluation of infinite series, many terms must be summed because the series

has oscillating behaviour. The series converges very slowly especially for strongly-sorbing media (large R_p), large spacing of two fractures (large S), and early time (small t). This could be one of the reasons why Sudicky and Frind have not shown any numerical results for M/N°. In Chapter 3 we will show a simplified analytical method for the evaluation of M/N° and its validity to overcome such difficulties.

2.2 Analytical Solutions for a Two-member Decay Chain in a Single Fracture

Sudicky and Frind[4] provided analytical solutions for the transport of a two-member decay chain through a single fracture (Fig. 2.2). Dispersion in the fracture is neglected because its effects were shown not to be important[1,2] and the solutions can be reduced to simpler functions. They considered an impulse release at the repository. Although general solutions for radioactive chains of more than two members can be derived by the same method, Sudicky and Frind have not obtained them because the solution form might be so complicated that the numerical evaluation is impractical.

In our previous report[6], we presented exact analytical solutions for an *n*-member decay chain, for any release mode, in recursive forms. From the standpoint of numerical evaluation, however, it is desirable to derive nonrecursive solutions, which is rather difficult for higher *n*. To ease the numerical evaluation, we neglected radioactive decay in the rock pores in previous calculations. In this section we will check the Sudicky and Frind's solutions and show how their solutions can be applied for obtaining the solutions for a general release.

The governing equations are:

$$\frac{\partial N_1}{\partial t} + \frac{v}{R_{f_1}} \frac{\partial N_1}{\partial z} + \lambda_1 N_1 + \frac{q_1}{bR_{f_1}} = 0, \qquad 0 < z < \infty, \; t > 0, \tag{2.23}$$

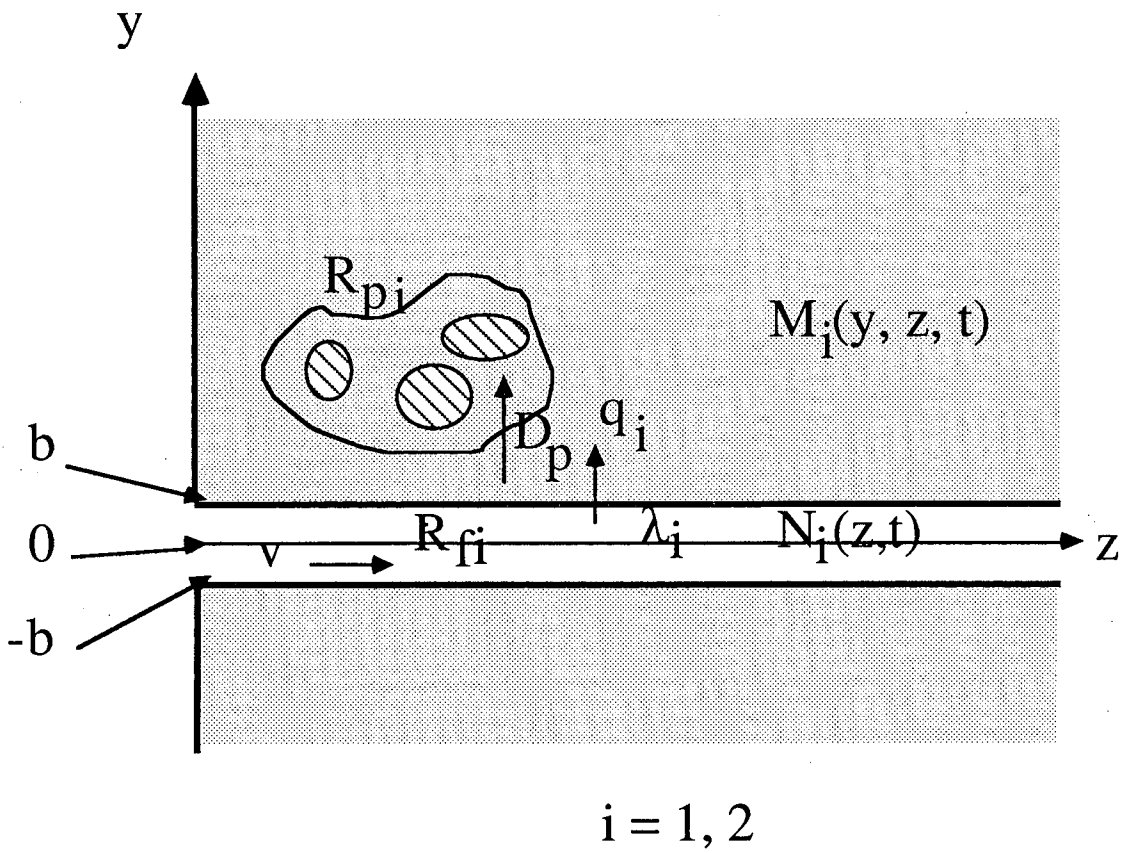

Fig. 2.2 A single fracture surrounded by a porous rock (the velocity v, the retardation coefficient R, the diffusion coefficient D, the rate of diffusion into the matrix q, porosity ε, and concentrations N(z,t), M(y,z,t). Subsctipts 1 and 2, f and p stand for the mother and the daughter nuclides, and fracture and pore, respectively)

$$\frac{\partial N_2}{\partial t} + \frac{v}{R_{f_2}} \cdot \frac{\partial N_2}{\partial z} + \lambda_2 N_2 - \frac{R_{f_1}}{R_{f_2}} \cdot \lambda_1 N_1 + \frac{q_2}{bR_{f_2}} = 0, \quad 0 < z < \infty, \quad t > 0, \tag{2.24}$$

$$\frac{\partial M_1}{\partial t} - \frac{D_{p_1}}{R_{p_1}} \cdot \frac{\partial^2 M_1}{\partial y^2} + \lambda_1 M_1 = 0, \qquad y > b, \quad z > 0, \quad t > 0, \tag{2.25}$$

$$\frac{\partial M_2}{\partial t} - \frac{D_{p_2}}{R_{p_2}} \cdot \frac{\partial^2 M_2}{\partial y^2} + \lambda_2 M_2 - \frac{R_{p_1}}{R_{p_2}} \cdot \lambda_2 M_2 = 0, \qquad y > b, \quad z > 0, t > 0, \tag{2.26}$$

where the nomenclature is as defined in the previous section. Subscripts 1 and 2 are for the mother and daughter nuclides, respectively. Dispersion in the fracture is neglected. The side conditions are:

$$N_i(z, 0) = 0, \qquad z > 0, \tag{2.27a}$$

$$M_i(y, z, 0) = 0, \qquad y > b, z > 0, \tag{2.27b}$$

$$N_i(0, t) = N_i^{\circ}\delta(t-0), \qquad t > 0, \tag{2.27c}$$

$$N_i(\infty, t) = 0, \qquad t > 0, \tag{2.27d}$$

$$M_i(b, z, t) = N_i(z, t), \qquad t > 0, z > 0, \tag{2.27e}$$

$$M_i(\infty, z, t) = 0, \qquad t > 0, z > 0, \tag{2.27f}$$

where i = 1,2 and $\delta(t)$ is a delta function. N_i°, i = 1, 2 are the strengths of the impulses at the repository at t = 0.

Sudicky and Frind apparently applied Laplace transforms for the governing equations and obtained the solutions. However, these solutions contain several apparently incorrect expressions as indicated in the following by boxes:

$$N_1(z, t) = N_1^{\circ} W_1(b, z, t), \qquad z \geq 0, t \geq 0, \tag{2.28}$$

$$M_1(y, z, t) = N_1^{\circ} W_1(y, z, t), \qquad y \geq b, z > 0, t \geq 0, \tag{2.29}$$

$$N_2(z, t) = N_1^{\circ} U_2(b, z, t) + N_2^{\circ} W_2(b, z, t), \qquad z \geq 0, t \geq 0, \tag{2.30}$$

$$M_2(y, z, t) = N_1^{\circ} \{ U_1(y, z, t) + U_2(y, z, t) \} + N_2^{\circ} W_2(y, z, t), \quad y \geq b, z > 0, t \geq 0, \tag{2.31}$$

where

$$W_i(y,z,t) = h(t-Z_iA_i)\frac{Z_i + B_i(y-b)}{2\sqrt{\pi}} E_i(Z_i + B_i(y-b),\, t-Z_iA_i)\cdot e^{-\lambda_i Z_i A_i}, \qquad i = 1, 2 \tag{2.32}$$

$$U_2(y,z,t) = \frac{\lambda_1\gamma_2}{4\pi}\int_0^z e^{-\frac{\lambda_1 R_{f_1}(z-\xi)}{v} - \frac{\lambda_2 R_{f_2}\xi}{v}} \int_0^{h(t-g)} E_1(\gamma_1(z-\xi),u)E_2(\gamma_2\xi+B_2(y-b),\, t-u-g)F(\xi,u;\, y,z,t)\,du\,d\xi, \tag{2.33}$$

$$E_i(\xi, u) = \frac{1}{\sqrt{u^3}}\cdot e^{-\frac{\xi^2}{4u} - \lambda_i u}, \qquad i = 1, 2, \tag{2.34}$$

$$F(\xi,u;\, y,z,t) = \frac{R_{f_1}\gamma_1\{\gamma_2\xi+B_2(y-b)\}(z-\xi)}{v\gamma_2} + \frac{R_{p_1}}{\sqrt{R_{p_2}D_{p_2}}}\left[\frac{\gamma_2 B_2(z-\xi)+B_1\{\gamma_2\xi+B_2(y-b)\}}{2\Phi} - \frac{B_1B_2\Theta}{4\Phi^2}\right.$$

$$+\sqrt{\frac{\pi}{\Phi}}\cdot e^{\frac{\Theta^2}{4\Phi}}\cdot \operatorname{erfc}\left[\frac{\Theta}{2\sqrt{\Phi}}\right]\cdot\left\{\frac{\gamma_1\{\gamma_2\xi+B_2(y-b)\}(z-\xi)}{2} - \frac{\Theta\{\gamma_1B_2(z-\xi)+B_1[\gamma_2\xi+B_2(y-b)]\}}{4\Phi}\right.$$

$$\left.\left. + \frac{B_1B_2\left(\frac{\Theta^2}{2}+\Phi\right)}{4\Phi^2}\right\}\right], \tag{2.35}$$

$$\gamma_i = \frac{\varepsilon}{bv\sqrt{D_{p_i}R_{p_i}}}, \qquad Z_i = \frac{R_{f_i}z}{vA_i}, \qquad A_i = \frac{bR_{f_i}}{\varepsilon\sqrt{D_{p_i}R_{p_i}}}, \qquad B_i = \sqrt{\frac{R_{p_i}}{D_{p_i}}}, \quad i = 1, 2, \tag{2.36}$$

$$g = \frac{R_{f_1}(z-\xi)}{v} + \frac{R_{f_2}\xi}{v}, \tag{2.37}$$

$$\Theta = \frac{\gamma_1 B_1(z-\xi)}{2u} + \frac{[\gamma_2\xi+B_2(y-b)]B_2}{2(t-u-g)}, \tag{2.38}$$

$$\Phi = \frac{B_1^2}{4u} + \frac{B_2^2}{4(t-u-g)}. \tag{2.39}$$

$U_1(y,z,t)$ has three different forms depending upon the parameter values:

(i) $B_1^2 \neq B_2^2$

$$U_1(y,z,t) = \frac{\lambda_1 R_{p_1}}{2D_{p_2}(B_2^2 - B_1^2)} \left\{ h(t-Z_1A_1) e^{-\lambda_1 t + \alpha(t-Z_1A_1)} \left[e^{-\sqrt{\alpha}[Z_1+B_1(y-b)]} \operatorname{erfc}\left[\frac{Z_1+B_1(y-b)}{2\sqrt{t-Z_1A_1}} - \sqrt{\alpha(t-Z_1A_1)} \right] \right.\right.$$

$$\left.\left. + e^{\sqrt{\alpha}[Z_1+B_1(y-b)]} \operatorname{erfc}\left[\frac{Z_1+B_1(y-b)}{2\sqrt{t-Z_1A_1}} + \sqrt{\alpha(t-Z_1A_1)} \right] \right] - \frac{B_2(y-b)}{4\sqrt{\pi}} h(t-Z_1A_1) \int_0^{t-Z_1A_1} \frac{1}{\sqrt{u^3}} \right.$$

$$\left. \cdot e^{-\lambda_1(t-u)+\alpha(t-Z_1A_1-u)} e^{-\frac{B_2^2(y-b)^2}{4u} - \lambda_2 u} \left[e^{-\sqrt{\alpha}Z_1} \operatorname{erfc}\left[\frac{Z_1}{2\sqrt{t-Z_1A_1-u}} - \sqrt{\alpha(t-Z_1A_1-u)} \right] + \right.\right.$$

$$\left.\left. e^{\sqrt{\alpha}Z_1} \operatorname{erfc}\left[\frac{Z_1}{2\sqrt{t-Z_1A_1-u}} + \sqrt{\alpha(t-Z_1A_1-u)} \right] \right] du \right\}, \quad y \geq b, \tag{2.40}$$

where

$$\alpha = \lambda_1 + \frac{B_1^2\lambda_1 - B_2^2\lambda_2}{B_2^2 - B_1^2}. \tag{2.41}$$

(2.40) is valid for negative α as well as non-negative α.

(ii) $B_1^2 = B_2^2$ and $\lambda_1 \neq \lambda_2$

$$U_1(y,z,t) = \frac{\lambda_1 D_{p_1}}{D_{p_2}(\lambda_2 - \lambda_1)} \left[W_1(y,z,t) - \frac{Z_1 B_1(y-b)}{4\pi} h(t-Z_1A_1) \int_0^{t-Z_1A_1} \frac{1}{\sqrt{u^3(t-Z_1A_1-u)^3}} e^{-\frac{Z_1^2}{4(t-Z_1A_1-u)} - \lambda_1(t-u)} \right.$$

$$\left. e^{-\frac{B_1^2(y-b)^2}{4u} - \lambda_2 u} du \right], \quad y \geq b. \tag{2.42}$$

(iii) $B_1^2 = B_2^2$ and $\lambda_1 = \lambda_2$

$$U_1(y,z,t) = \lambda_1 B_1(y-b) \frac{D_{p_1}}{D_{p_2}} \cdot \frac{1}{2\sqrt{\pi}} \cdot h(t-Z_1A_1) \cdot (t-Z_1A_1) \cdot E_1(Z_1 + B_1(y-b), t-Z_1A_1) e^{-\lambda_1 Z_1 A_1}. \tag{2.43}$$

The Heaviside step function which comes from the identity (2.13) has been ignored

in several places. When Sudicky and Frind took the inverse Laplace transform of the term,

$$e^{-B_2(y-b)\sqrt{p+\lambda_2}},$$

which exists in the Laplace-transformed solution for $U_1(y, z, t)$, they apparently made use of the identity:

$$L^{-1}\left[e^{-k\sqrt{p}}\right] = \frac{k}{2\sqrt{\pi t^3}} e^{-\frac{k^2}{4t}}, \tag{2.44}$$

which is valid[8] only for $k > 0$. In their case $k = B_2(y-b)$. Therefore, $U_1(y, z, t)$ is applicable in the region $y > b$; and the solution for $M_2(y, z, t)$, $\lambda_1 \neq \lambda_2$, does not satisfy the boundary condition (2.27e). This difficulty can be avoided by considering the limit:

$$\lim_{\substack{t\to 0 \\ k\to 0}} \left[\frac{k}{2\sqrt{\pi t^3}} \cdot e^{-\frac{k^2}{4t}}\right] = \delta(t - 0). \tag{2.45}$$

Another way is to regroup the terms in $\tilde{U}_1(y, z, p)$, the Laplace transformed U_1, and to apply the identity:

$$L^{-1}\left[\frac{1}{p-a} \cdot e^{-k\sqrt{p}}\right] = \frac{1}{2}e^{at}\left[e^{-k\sqrt{a}}\operatorname{erfc}\left\{\frac{k}{2\sqrt{t}} - \sqrt{at}\right\} + e^{k\sqrt{a}}\operatorname{erfc}\left\{\frac{k}{2\sqrt{t}} + \sqrt{at}\right\}\right] \tag{2.46}$$

which is valid for $k \geq 0$.

From the standpoint of numerical evaluation there are two major difficulties in their solutions: to perform the double integral in $U_2(y,z,t)$ and to evaluate the complementary error function erfc(z) for a complex value z , which occurs in the case $\lambda_1 < \lambda_2$. The latter requires the summation of infinite series[8]:

$$\operatorname{erf}(x+iy) = \operatorname{erf}(x) + \frac{e^{-x^2}}{2\pi x}\{(1 - \cos 2xy) + i\sin 2xy\} + \frac{2}{\pi}e^{-x^2}\sum_{n=1}^{\infty}\frac{e^{-\frac{n^2}{2}}}{n^2 + 4x^2}\{f_n(x,y) + ig_n(x,y)\} + (\text{remainder}),$$

where

$$f_n(x, y) = 2x - 2x\cdot\cosh(ny)\cdot\cos(2xy) + n\cdot\sinh(ny)\cdot\sin(2xy),$$

$$g_n(x, y) = 2x\cdot\cosh(ny)\cdot\sin(2xy) + n\cdot\sinh(ny)\cdot\sin(2xy),$$

i is the imaginary unit, x , y real. (2.47)

By using the solutions (2.28) to (2.31), we can write the solutions for a general release:

$$N_i(0, t) = \psi_i(t), \qquad i = 1, 2, \qquad t > 0, \tag{2.48}$$

by taking the convolution of $\psi_i(t)$ and $W_1(y,z,t)$, $W_2(y,z,t)$, $U_1(y,z,t)$, and $U_2(y,z,t)$ with respect to time:

$$N_1(z, t) = \int_0^t \psi_1(t-\tau) W_1(b, z, \tau) d\tau, \tag{2.49}$$

$$M_1(y, z, t) = \int_0^t \psi_1(t-\tau) W_1(y, z, \tau) d\tau, \tag{2.50}$$

$$N_2(z, t) = \int_0^t \psi_1(t-\tau) U_2(b, z, \tau) d\tau + \int_0^t \psi_2(t-\tau) W_2(b, z, \tau) d\tau, \tag{2.51}$$

$$M_2(y, z, t) = \int_0^t \psi_1(t-\tau) \{U_1(y, z, \tau) + U_2(y, z, \tau)\} d\tau + \int_0^t \psi_2(t-\tau) W_2(y, z, \tau) d\tau, \tag{2.51}$$

which means that $U_i(z, t)$, $W_i(y, z, t)$ i = 1, 2 can be used as Green's functions. In Chapter 4 we make numerical evaluations for $N_i(z, t)$ with $\psi_i(t)$ obeying the Bateman equations, and compare the results with our previous evaluation obtained by neglecting the decay in the porous rock.

3. Superposition Approximation for Parallel Fracture System

As shown in Section 2.1, the exact solutions for a system of parallel fractures are rather complicated, and no numerical evaluations for the concentration in the rock pores were given by Sudicky and Frind. Here we show the numerical results of the concentration in the rock pores by applying a simplified analytical method that superposes single-fracture solutions. And we consider the validity of the superposition approximation.

3.1 Formulations

Consider the system of parallel fractures depicted in Fig. 2.1. Single-fracture solutions have been derived based upon the assumption that the fracture spacing is such that there is no overlap of two concentration fields produced by the adjacent fractures. If the contaminant penetrates so deeply into the rock matrix that concentration fields from adjacent fractures overlap, consideration of multiple fractures in predicting contaminant transport is required. However, the single-fracture solutions are applicable if the overlap is acceptably small. In Figure 3(a), the overlap of two profiles in the rock matrix is almost negligible. This means that the single-fracture solutions satisfy the boundary condition, (2.6e), at the rock/fracture interface with negligible errors. This situation will occur if it is early time, if the rock has strong sorption capacity, if the diffusion coefficient is small, or if the spacing of two fractures is large. In Figure 3(b), on the contrary, the overlap is significant. The influence of the adjacent fractures is so large that the boundary condition, (2.6e), is no longer satisfied by the single-fracture solutions. This situation will occur in cases of long time, weakly-sorbing rock, large diffusion coefficients, or small spacings. In the former case, we can approximate the concentration in the rock pores by superposing two profiles:

$$M_t(y, z, t) = M(y, z, t) + M(2S-y, z, t) \tag{3.1}$$

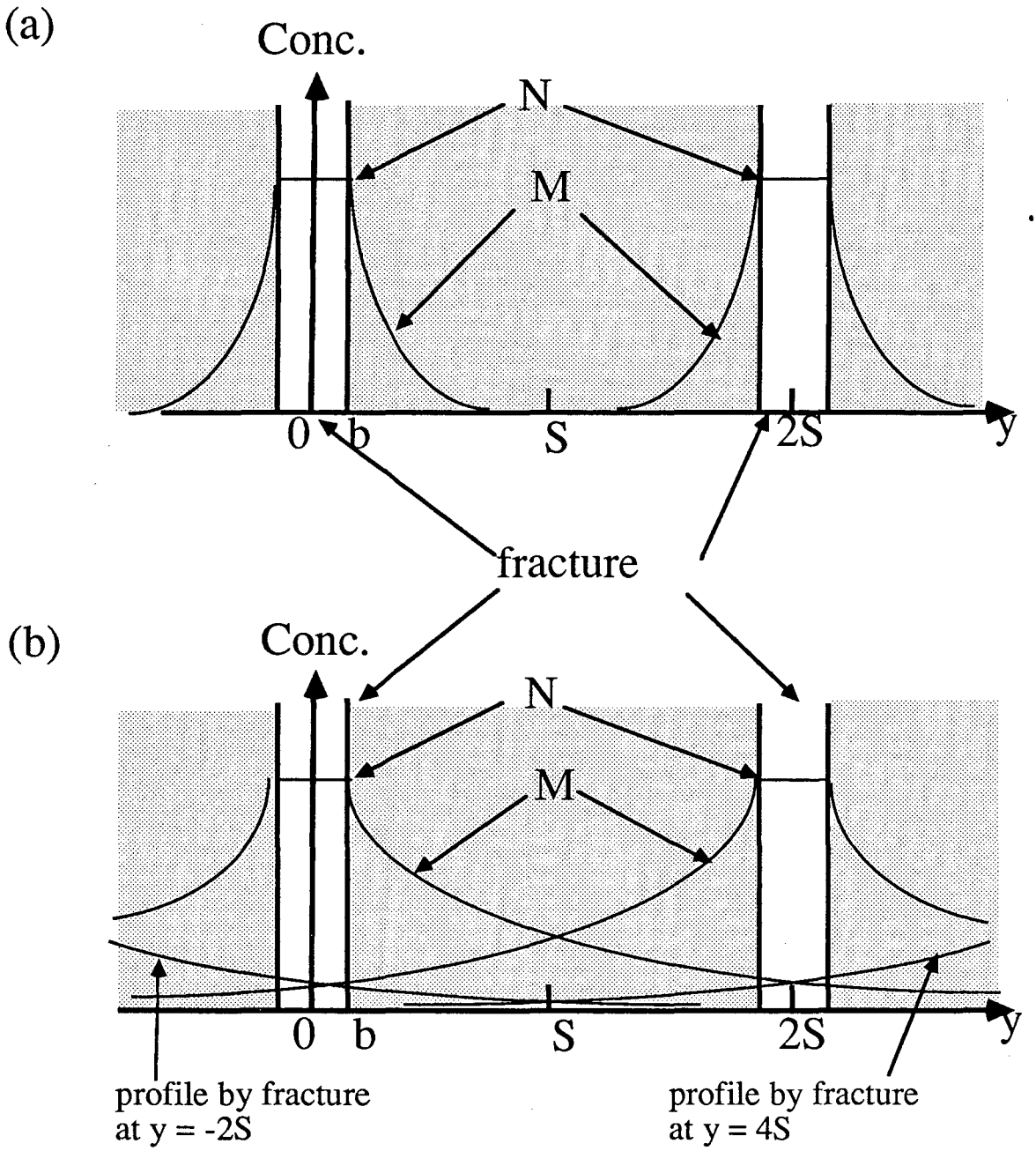

Fig. 3.1 Illustration of the overlap of two concentration fields. The top figure depicts valid superposition, which occurs in cases of small t and D_p and large R_p and S. The bottom figure shows invalid superposition. Note that, in the bottom figure, significant overlap takes place such that the profile by each fracture shows considerably large concentration beyond its adjacent fractures.

where $M_t(y, z, t)$ is the approximation of the concentration in the rock pores for finite fracture spacing, 2S, and M(y, z, t) is the single-fracture solution. (For M(y, z, t), several analytical solutions have been obtained[1,2,6] depending on the source boundary conditions and the presence of the dispersion in the fracture.)

Based upon the above observation, we impose the condition for valid superposition solutions :

$$\frac{M(2S-b,\, z,\, t)}{M(b,\, z,\, t)} \leq 0.01, \tag{3.2}$$

so that the influence of the concentration field by the neighboring fracture is less than one percent of the concentration produced by the fracture of interest (Fig. 3.2). Then the boundary condition at y = b can be satisfied by the single-fracture solutions within 1 percent accuracy.

This condition can be expressed more clearly in terms of the Fourier number,

$$F = \frac{D_p}{R_p} \cdot \frac{t}{(2S)^2}. \tag{3.3}$$

The Fourier number measures the time in which the diffusion process is continuing. A large Fourier number means that long time has passed since the diffusion process started. Hence, the diffusion front has penetrated deeply into the medium.

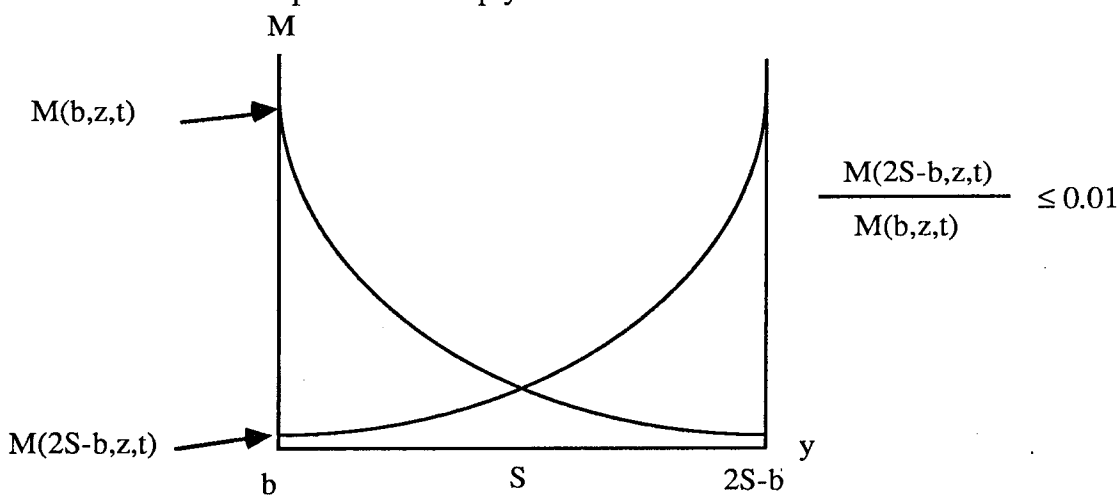

Fig. 3.2. Illustration of the validity condition imposed on the single-fracture solution.

Turning to our problem, since thevalid superposition can be interpreted as shallow penetration by diffusion, we could find an upper bound of the Fourier number for a valid superposition. Since taking a large D_p or a small 2S is equivalent to taking a small R_p, we survey the range of the Fourier number, where (3.2) is satisfied, by changing t and R_p, fixing the values of D_p and 2S, and express the validity domain in (t, R_p) space. This validity domain can be expressed by an inequality for t/R_p:

$$\frac{t}{R_p} \leq \beta, \tag{3.4}$$

where β is a constant obtained from the numerical evaluations. Then the condition which the Fourier number must satisfy becomes:

$$F \leq \frac{D_p}{(2S)^2} \cdot \beta . \tag{3.5}$$

To illustrate, we consider the step and band releases for the boundary concentration at z = 0 in the fractures:

$$\psi(t) = N^o e^{-\lambda t} h(t), \quad \text{and} \tag{3.6a}$$

$$\psi(t) = N^o e^{-\lambda t} \{h(t) - h(t-T)\}, \tag{3.6b}$$

where T is the leach time and h(t) is a Heaviside step function. We do not consider the dispersion in the fracture because its effect is negligible[1] for expected values of the dispersion coefficient. Then the single-fracture solutions, M(y, z, t), for (3.2a) and (3.2b) can be written as[1]:

$$M(y, z, t) = f_1(y, z, t), \qquad \text{for a step release} \tag{3.7a}$$

$$M(y, z, t) = f_1(y, z, t) - e^{-\lambda T} f_1(y, z, t - T), \qquad \text{for a band release} \tag{3.7b}$$

respectively, where

$$f_1(y, z, t) = N^o h(t - ZA)\, e^{-\lambda t} \operatorname{erfc}\left[\frac{Z + B(y-b)}{2\sqrt{t - ZA}}\right] \tag{3.8}$$

$$Z = \frac{R_f z}{vA}, \qquad A = \frac{bR_f}{\varepsilon\sqrt{D_p R_p}}, \qquad B = \sqrt{\frac{R_p}{D_p}}. \tag{3.9}$$

The nomenclature is the same as defined in Section 2.1.

3.2 Validity of the Superposition Approximation

We calculate the single-fracture solution, M(y, z, t) at y = b and y = 2S - b for R_p and t ranging from 1 to 10^3 and from 10^2 to 10^7 years, respectively, with the common parameter values:

$z = 1, 10^2, 10^4$ m,	$v = 10$ m/yr
$\varepsilon = 0.01$,	$2b = 0.01$ m
$D_p = 0.01$ m^2/yr,	$R_f = 1$
$\lambda = 3.24 \times 10^{-7}$ 1/yr,	T = 30,000 yr for band release.

We performed numerical calculations for ^{237}Np. Because of the imposed condition for validity (3.2), the decay constant does not affect the validity. (The factor $\exp(-\lambda t)$ in $f_1(y, z, t)$ cancels when (3.7a,b) are substituted into (3.2).)

The inequality (3.2) is checked at z = 1, 10^2, and 10^4 m for various (t, R_p) points, resulting in Fig. 3.3. This figure shows the domain of (t, R_p) that satisfies (3.2). Superposition is valid to the left of each line. For a band release there is a stepwise change at the end of the leach time; thereafter the constraints on t and R_p are more limited. For large z the change at the end of the leach time is small, and at z = 10^4 m the stepwise change disappears. For a step release t/ R_p must be smaller than 3000 yr for z = 1 m and z = 10^2 m and smaller than 8000 yr for z = 10^4 m. From (3.3), therefore, the Fourier number must be less than 0.075 for z = 1 m and 10^2 m and can be as large as 0.2 for z = 10^4 m. For a band release and at times greater than the leach time, we require F ≤ 0.02 for z = 1 m, 0.033 for z = 10^2 m, and 0.2 for z = 10^4 m. Different constraints on F will be obtained for different R_f values. One can see the advantage of the approximation method from this figure. The exact solutions obtained by Sudicky and Frind require the summation of an infinite series, which converges very slowly especially at early times. However, it is in the early time region that

the approximation is valid regardless of R_p values.

We can confirm the observation in Fig.3.3 by calculating the actual concentration profiles in the rock matrix for several t and R_p values with a step or a band release, which are depicted in Figs. 3.4 to 3.6. In Table 3.1, summarized are the calculation conditions and the validity of the resultant profiles. Figure 3.4 shows the calculated concentration profiles for $z = 10^2$ m, a step release. One can observe that the concentration profile is extending into the rock matrix as time increases. The three early time profiles yield valid superposition; the later profile shows considerable overlap from adjacent fractures, resulting in invalid superposition.

Figure 3.5 shows the concentration profiles calculated for $z = 10^2$ m, $R_p = 10^2$, a band release. As can be deduced from Fig. 3.3, with $t = 2 \times 10^5$ yr and $R_p = 10^2$ the superposition is valid for a step release, but not for a band release. Before and after the end of the leach time, the concentration in the fractures decreases quickly. So does the concentration at the rock/fracture interface by the boundary condition, (2.6e), i.e., M(b,z,t) = N(z,t). Then the concentration profile in the rock produced by each fracture has a maximum in the y-direction. Because the denominator of the condition (3.2) becomes smaller after the leach time, it becomes more difficult to meet the condition (3.2), and the constraint on the Fourier number becomes more limited. Two early time profiles yield valid superposition. At $t = 10^4$ yr, the profile is the same as that for the step release (see Fig. 3.4). At $t = 6 \times 10^4$ yr, greater than the leach time, the superposed profile shows two peaks in the y-direction because the two fracture-induced profiles, each of which has a maximum in the y-direction, are about to overlap at the midpoint (y = 10 m). Two later profiles show invalid superposition. At $t = 2 \times 10^5$ yr and 10^6 yr, the fracture-induced profiles become very broad, and the diffusion front of each profile exceeds the adjacent fracture location. We can no longer distinguish the peak of each fracture-induced profile in the superposed profile. Thus the single-peak superposed profile implies invalid superposition.

Figure 3.6 shows the concentration profiles calculated for $z = 10^2$ m, $R_p = 2$, for

both band and step releases. Before the end of the leach time, both release modes give the same profiles ($t = 2 \times 10^3$ yr and 10^4 yr). The superposition becomes invalid even before the leach time (at $t = 10^4$ yr). At $t = 10^5$ yr, greater than the leach time, for a step release, the concentration at the rock/fracture interface is significantly higher than unity. This means at once invalid superposition because the maximum probable concentration is unity. For a band release, we observe a single-peak profile, which means invalid superposition.

Table 3.1 Calculation conditions and validity of resultant profiles

Figure	Distance (z), m	Leach time (T), year	Release mode $\psi(t)$	Pore Retardation (R_p)	Time (t), year	Superposition technique valid or invalid(1)
3.4	100	-----(2)	Step	100	1×10^4	VALID
					6×10^4	VALID
					2×10^5	VALID(3)
					1×10^6	NOT VALID
3.5	100	30,000	Band	100	1×10^4	VALID
					6×10^4	VALID
					2×10^5	NOT VALID(3)
					1×10^6	NOT VALID
3.6	100	30,000(4)	Step/Band	2	2×10^3	VALID
			Step/Band	2	1×10^4	NOT VALID
			Step	2	1×10^5	NOT VALID
			Band	2	1×10^5	NOT VALID

Note:
(1) Validity is judged by Fig. 3.3.
(2) For a step release, the leach time can be considered infinite.
(3) These two show that the constraint for valid superposition is more limited for a band release than for a step release.
(4) Before the leach time (30,000yr), the profiles are identical for both release modes. After the leach time, (1×10^5 yr is the only case), they becomes different, but both of them are invalid superposition.

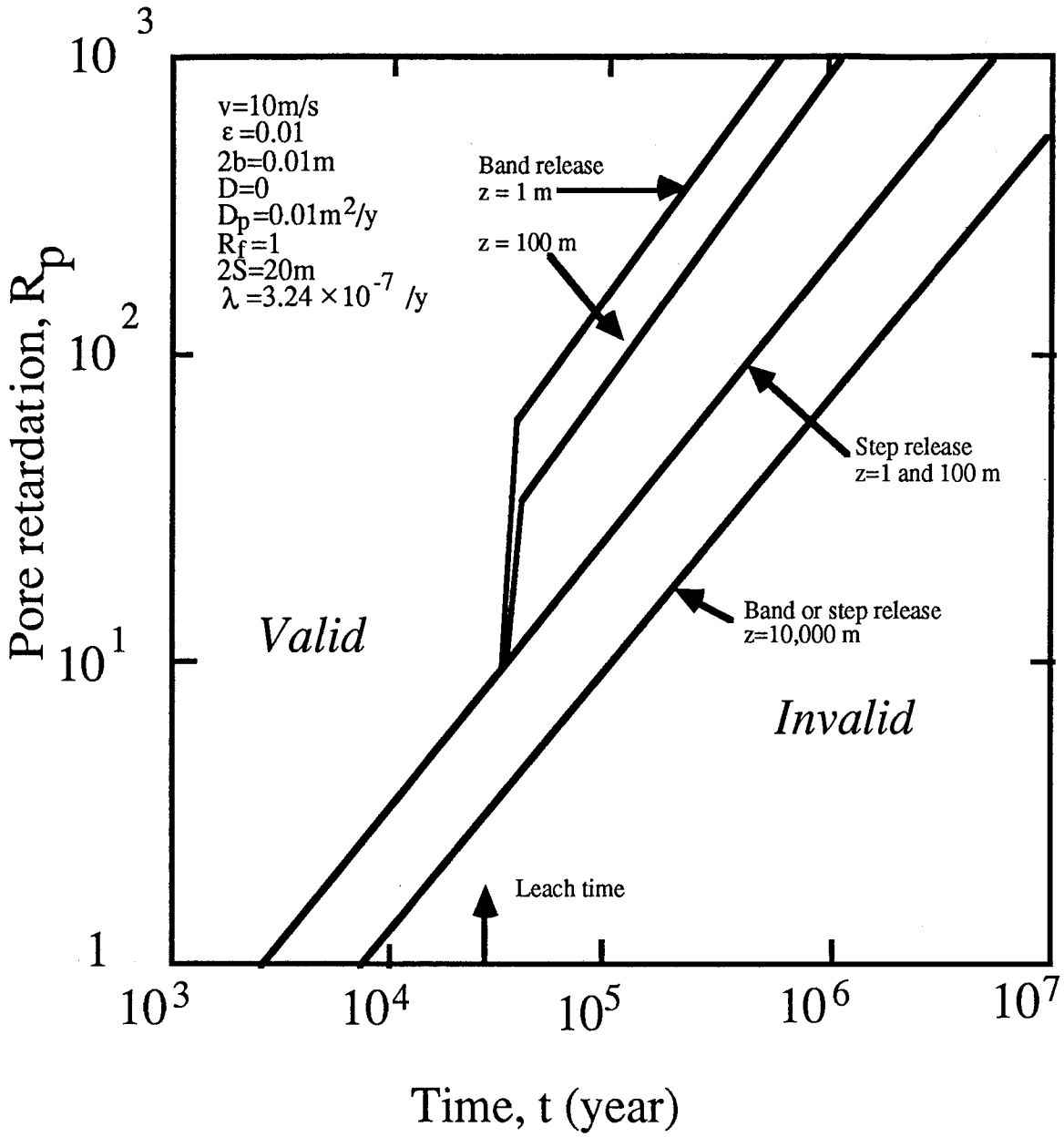

Fig. 3.3 Validity domain for superposed solutions, step and band releases

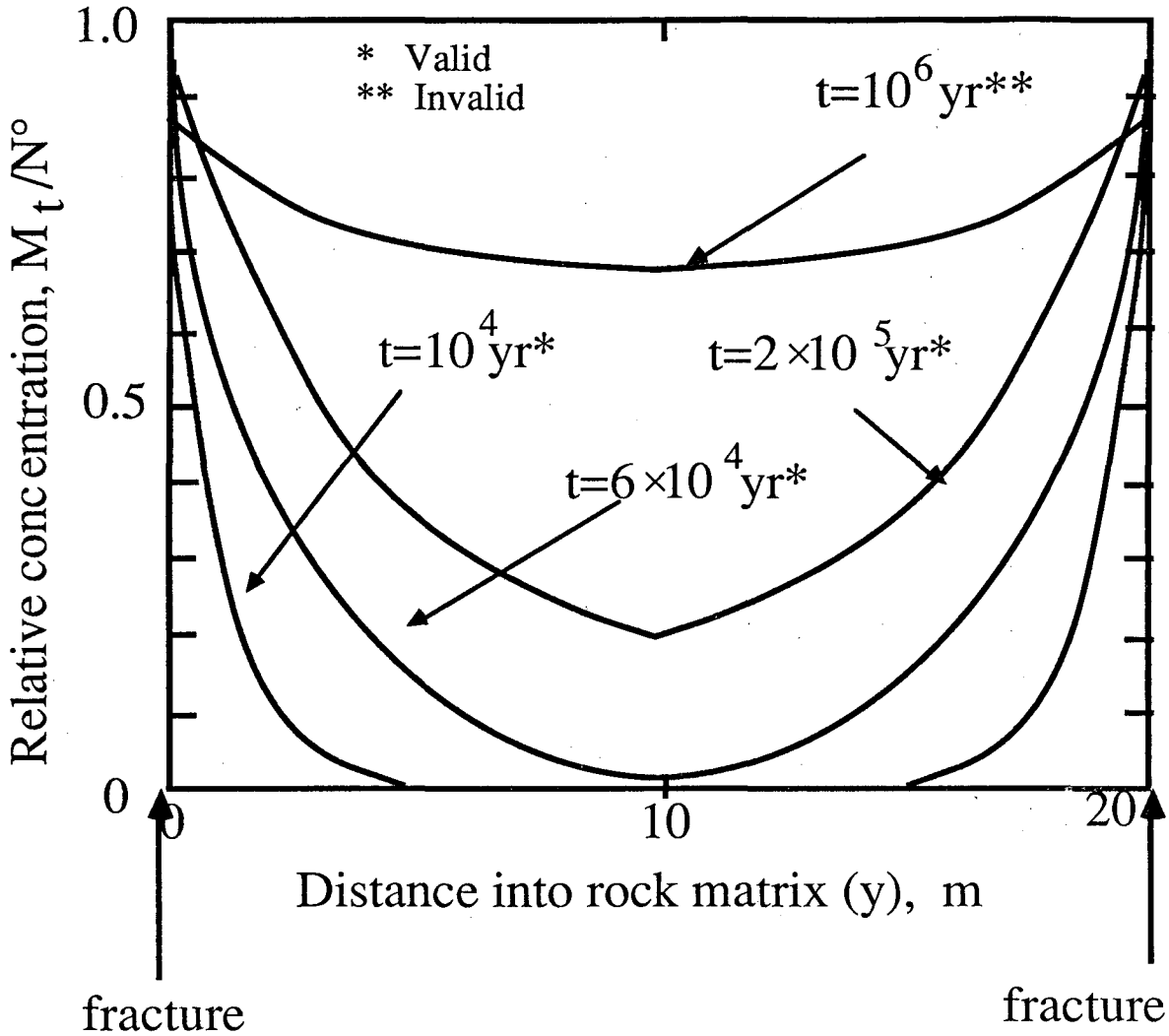

N°: the initial concentration at t he repository

Fig. 3.4 Concentration profiles in the rock matrix (z=100 m, R_p= 100), a step release.

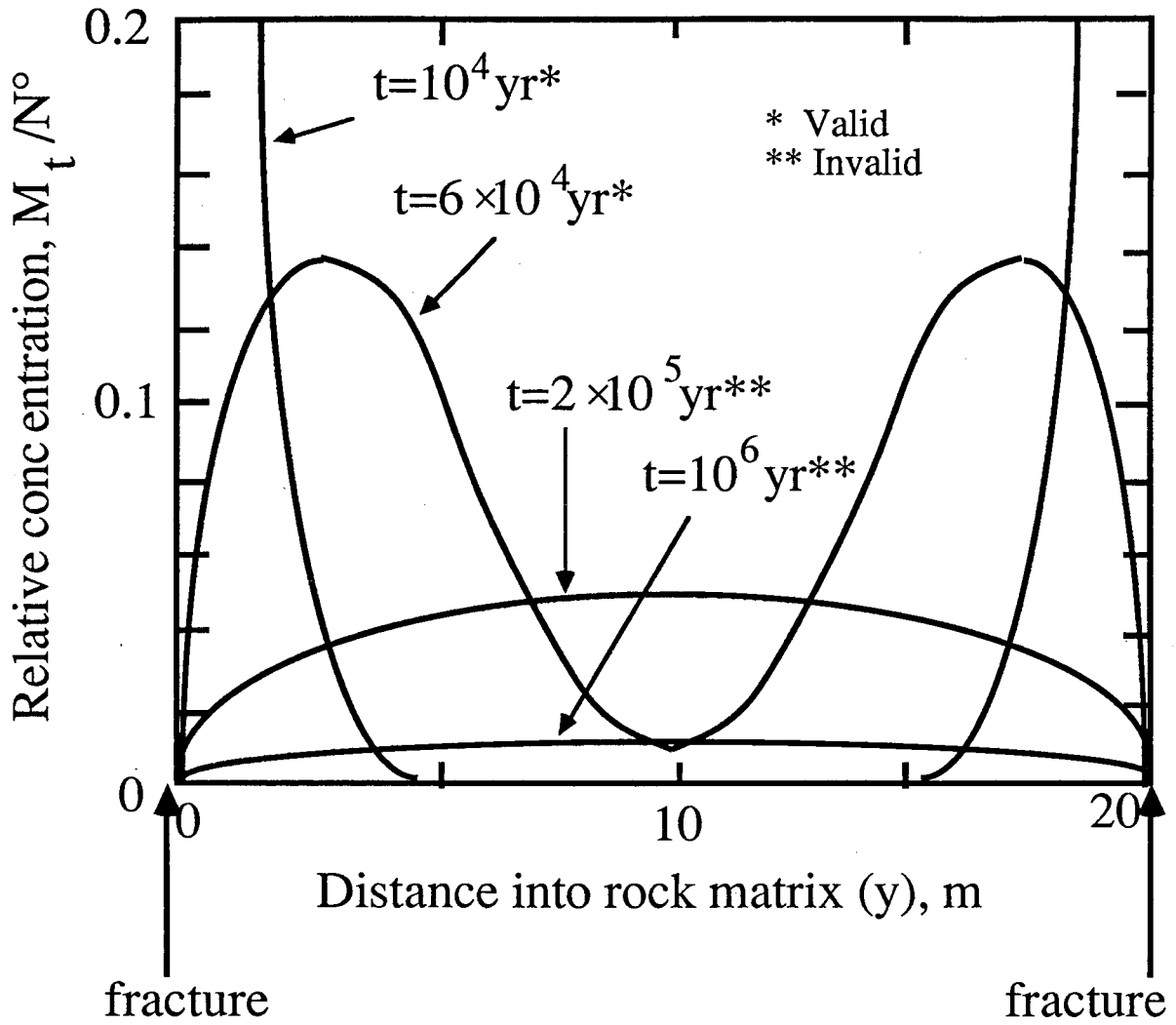

N°: the initial concentration at t he repository

Fig. 3.5 Concentration profiles in the rock matrix (z = 100 m, R_p = 100), a band release with a leach time of 30,000 yr

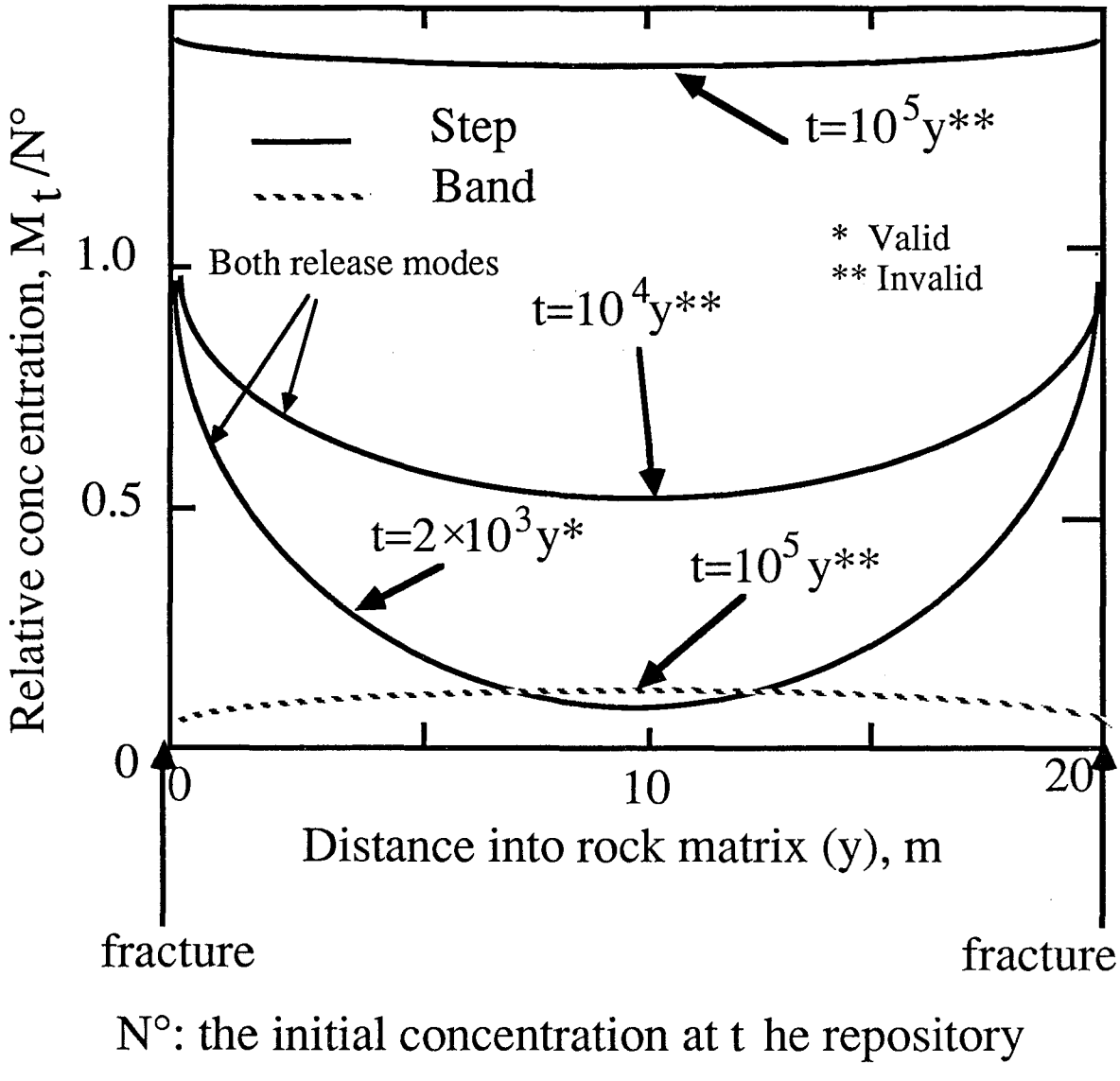

Fig. 3.6 Concentration profiles in the rock matrix (z=100 m, R_p = 2), step and band releases (T = 30,000 yr). Before t = 30,000 yr both release modes give the same profiles

4. Numerical Evaluation of the Solutions for a Two-Member Decay Chain with a Step Release

4.1 Formulations

We consider here the problem described through (2.23) to (2.27f) for a general release mode. The governing equations and side conditions are:

$$\frac{\partial N_1}{\partial t}+\frac{v}{R_{f_1}}\cdot\frac{\partial N_1}{\partial z}+\lambda_1 N_1+\frac{q_1}{bR_{f_1}}=0, \qquad 0<z<\infty,\ t>0, \tag{4.1}$$

$$\frac{\partial N_2}{\partial t}+\frac{v}{R_{f_2}}\cdot\frac{\partial N_2}{\partial z}+\lambda_2 N_2-\frac{R_{f_1}}{R_{f_2}}\cdot\lambda_1 N_1+\frac{q_2}{bR_{f_2}}=0,\ 0<z<\infty,\ t>0, \tag{4.2}$$

$$\frac{\partial M_1}{\partial t}-\frac{D_{p_1}}{R_{p_1}}\cdot\frac{\partial^2 M_1}{\partial y^2}+\lambda_1 M_1=0, \qquad y>b,\ z>0,\ t>0, \tag{4.3}$$

$$\frac{\partial M_2}{\partial t}-\frac{D_{p_2}}{R_{p_2}}\cdot\frac{\partial^2 M_2}{\partial y^2}+\lambda_2 M_2-\frac{R_{p_1}}{R_{p_2}}\cdot\lambda_2 M_2=0, \qquad y>b,\ z>0, t>0, \tag{4.4}$$

subject to the side conditions:

$$N_i(z,0)=0, \qquad z>0, \tag{4.5a}$$

$$M_i(y,z,0)=0, \qquad y>b,\ z>0, \tag{4.5b}$$

$$N_i(0,t)=\psi_i(t), \qquad t>0, \tag{4.5c}$$

$$N_i(\infty,t)=0, \qquad t>0, \tag{4.5d}$$

$$M_i(b,z,t)=N_i(z,t), \qquad t>0,\ z>0, \tag{4.5e}$$

$$M_i(\infty,z,t)=0, \qquad t>0,\ z>0, \tag{4.5f}$$

where $\psi_i(t)$, i = 1, 2 express the general release at the repository. Dispersion in the fracture is neglected. This problem can be solved by considering the subsidiary problem where the boundary condition (4.5c) is replaced by

$$N_i(0,t)=\delta(t-0) \tag{4.6}$$

We write the solutions of the subsidiary problem, $N_i^g(z,t)$ and $M_i^g(y,z,t)$, by setting $N^\circ_1 = N^\circ_2 = 1$ in eqs. (2.28) to (2.31), as:

$$N_1^g(z, t) = W_1(b, z, t), \qquad z \geq 0, t \geq 0, \tag{4.7}$$

$$M_1^g(y, z, t) = W_1(y, z, t), \qquad y \geq b, z > 0, t \geq 0, \tag{4.8}$$

$$N_2^g(z, t) = U_2(b, z, t) + W_2(b, z, t), \qquad z \geq 0, t \geq 0, \tag{4.9}$$

$$M_2^g(y, z, t) = U_1(y, z, t) + U_2(y, z, t) + W_2(y, z, t), \qquad y \geq b, z > 0, t \geq 0, \tag{4.10}$$

where $U_1(y,z,t)$, $U_2(y,z,t)$, $W_1(y,z,t)$, and $W_2(y,z,t)$ have been defined in Section 2.2. Then, solutions to the original problem can be obtained by applying the convolution theorem with respect to time:

$$N_1(z, t) = \int_0^t \psi_1(t-\tau) W_1(b, z, \tau) d\tau, \tag{4.11}$$

$$M_1(y, z, t) = \int_0^t \psi_1(t-\tau) W_1(y, z, \tau) d\tau, \tag{4.12}$$

$$N_2(z, t) = \int_0^t \psi_1(t-\tau) U_2(b, z, \tau) d\tau + \int_0^t \psi_2(t-\tau) W_2(b, z, \tau) d\tau, \tag{4.13}$$

$$M_2(y, z, t) = \int_0^t \psi_1(t-\tau) \{U_1(y, z, \tau) + U_2(y, z, \tau)\} d\tau + \int_0^t \psi_2(t-\tau) W_2(y, z, \tau) d\tau, \tag{4.14}$$

To illustrate, we take the step release for two members for $\psi_i(t)$:

$$\psi_1(t) = N_1^o h(t) e^{-\lambda_1 t}, \tag{4.15}$$

$$\psi_2(t) = N_2^o h(t)\, e^{-\lambda_2 t} + \frac{N_1^o \lambda_1 h(t)}{\lambda_2 - \lambda_1} \cdot \left\{ e^{-\lambda_1 t} - e^{-\lambda_2 t} \right\}. \tag{4.16}$$

4.2 Results and Discussions

In the previous report[6] we showed the results of an approximate model neglecting radioactive decay in (4.2) and (4.4). It has been shown that for the mother nuclide of the three-member chain the approximation gives fairly good results for the concentration in the

fracture for long half-life mother nuclides such as ^{237}Np and ^{234}U. But there has been no demonstration of the accuracy of the results for the daughter nuclides. We compare the results obtained by the exact model, i.e., (4.11) and (4.13) with those of the approximate model.

Figure 4.1 shows the concentration in the fracture for the $^{237}Np \rightarrow {}^{233}U$ chain with a step release at t = 10,000 yr. Parameter values are shown in the figure. For ^{237}Np the approximate and exact solutions give the almost same results, while for ^{233}U the approximation has introduced considerable error at a distance from the source with the approximate results different from the exact ones by several orders of magniture. There is a discontinuity in the ^{233}U profile at z = 100 m, which results from the two contributions: the ^{233}U generated at the repository and the ^{233}U generated in the medium. The former forms the near-field plateau and the latter the far-field plateau in the concentration profile. The neglected terms in the governing equation (4.4) for the concentration M_2 would have given the positive contribution at far field because

$$\lambda_1 R_{p1} M_1 - \lambda_2 R_{p2} M_2 = 0.0000324 M_1 - 0.0642 M_2$$

and M_1 is about 10^4 times larger than M_2. The orders of M_1 and M_2 can be roughly estimated from those of N_1 and N_2 in the figure. Therefore, neglecting the decay chain in the rock matrix makes the concentration in the rock pores lower, resulting in the overestimated gradient and diffusion flow at the rock/fracture interface. Thus the concentration of ^{233}U in the fracture has been underestimated by neglecting the decay in the rock matrix.

Figure 4.2 shows the concentration in the fracture for the $^{234}U \rightarrow {}^{230}Th$ chain with a step release at t = 10,000 yr. Parameter values are shown in the figure. Also in this case the approximation gives smaller results that the exact at far field. The neglected terms in the governing equation (4.4) for M_2 would have given the positive contribution because

$$\lambda_1 R_{p1} M_1 - \lambda_2 R_{p2} M_2 = 0.04215 M_1 - 0.433 M_2$$

and M_1 is about 30 times larger than M_2. Then by the same argument it can be said that the concentration of ^{230}Th in the fracture is underestimated by neglecting decay in the rock.

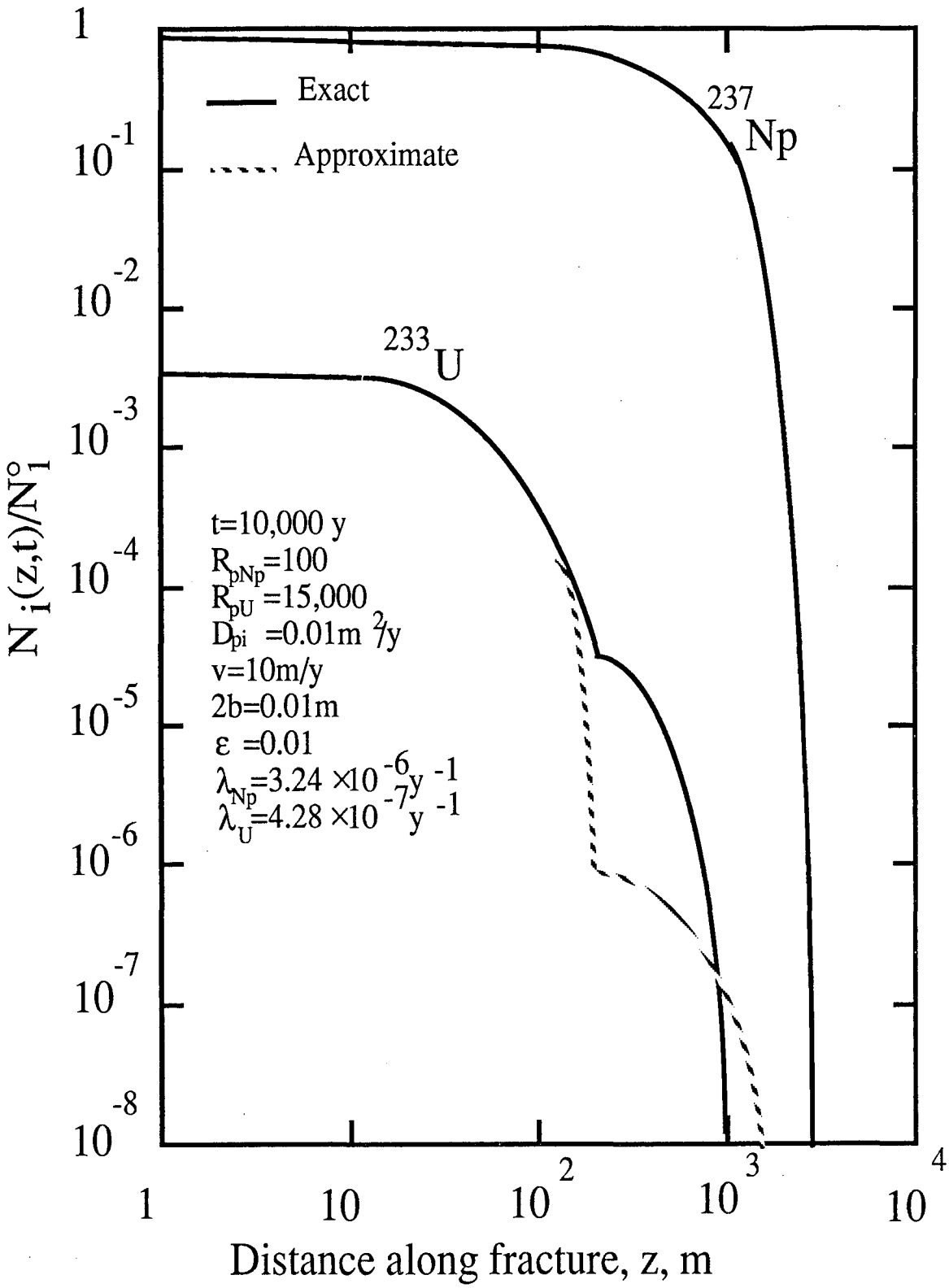

Fig. 4.1 Concentration profiles at t = 10,000 yr for $^{237}Np \rightarrow {}^{234}U$ chain, from a step release.

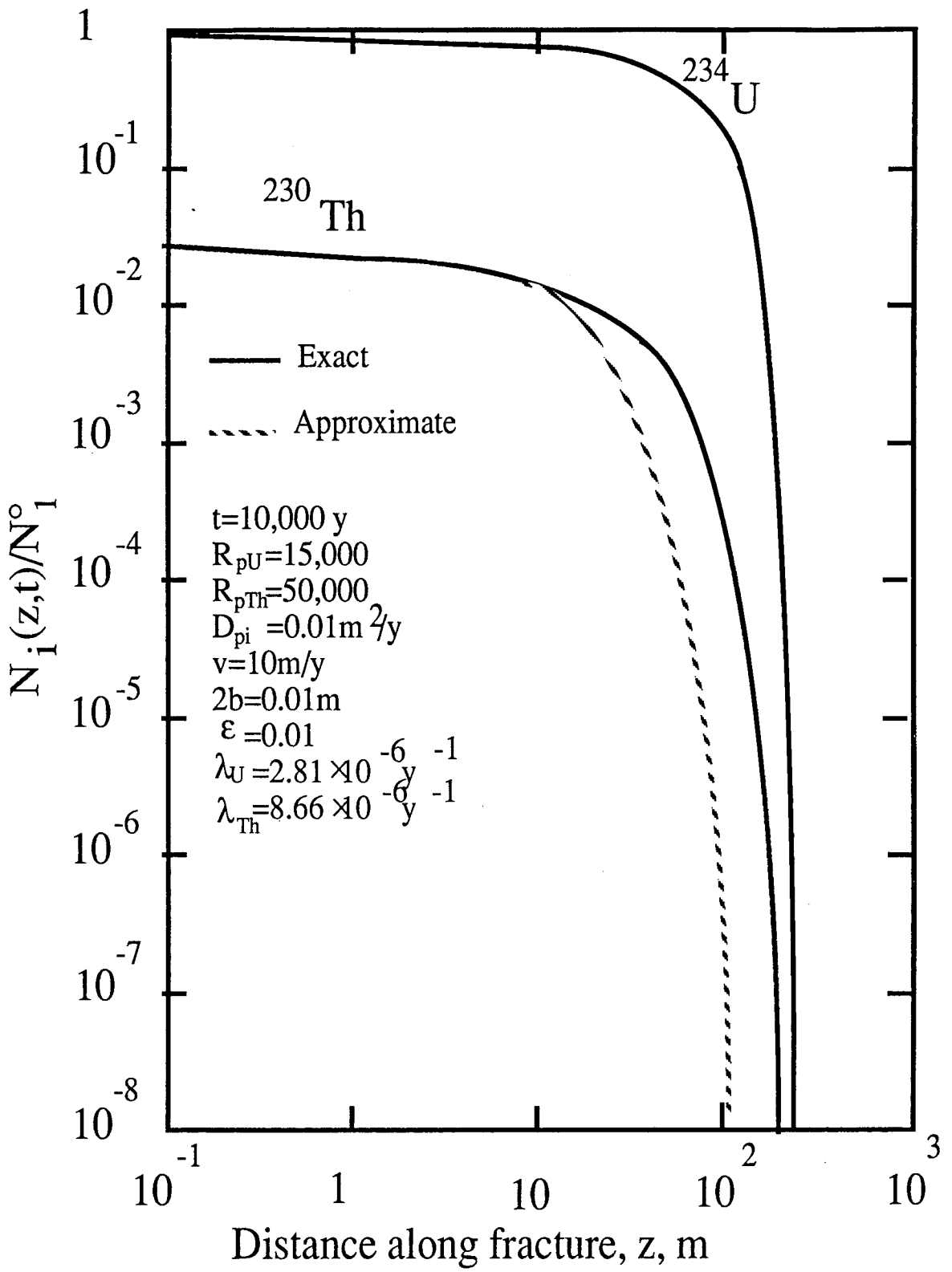

Fig. 4.2 Concentration profiles at t = 10,000 yr for $^{234}U \rightarrow {}^{230}Th$ chain, from a step release.

5. Concluding Remarks

We presented in this report the analytical study of the radionuclide transport through fractured, porous rock. Based upon the previous studies, where radionuclide transport was intensively studied on the assumptions of a single planar fracture and no precursors, we studied the analytical methods to evaluate the time-space-dependent concentrations for multiply-fractured rock and a two-member decay chain.

For multiply-fractured rock, we checked Sudicky and Frind's analytical solutions, and found apparently incorrect expressions. We gave the corrected versions of their solutions. The exact analytical solutions, however, require a summation of an infinite series and multiple integrations. The convergence of the infinite series is quite slow in case of shallow penetration into the rock matrix. We showed the superposition method to evaluate the concentration in the rock matrix. Solutions for multiply fractured rock are obtained by superposing two single-fracture solutions. The superposed solution gives fairly good approximation in case of shallow penetration into the rock matrix, for which numerical evaluation is difficult with the exact solutions. The constraint for valid superposition was given in terms of Fourier number. By this method we could extend the applicability of the single-fracture solutions.

For a two-member decay chain, we showed the solutions for a general release mode in the form of the convolution integrals of the release characteristics functions and the Green's functions. Sudicky and Frind obtained the solutions for an impulse release, which contain apparent by incorrect expressions. We corrected their solutions, and derived the Green's functions for this problem from Sudicky and Frind's solutions. Numerical evaluation was performed for an exponentially decaying step release. The convolution integrals were numerically evaluated by Gauss quadratures. This results were compared with our previous numerical results approximated by neglecting decay in the rock matrix. We found that for the mother nuclide the exact and the approximate solutions give very close results, while for

the daughter nuclide, the approximation introduces considerable errors at far field from the repository.

6. References

1 Ahn, J., P. L. Chambré, T. H. Pigford, "Nuclide Migration through a Planar Fissure with Matrix Diffusion", LBL-19429, April, 1985

2 Tang, D. H., E. O. Frind, and E. A. Sudicky, "Contaminant transport in Fractured Porous Media: Analytical Solution for a Single Fracture", Water Resour. Res., 17, 555-564, 1981

3 Sudicky, E.A. and E. O. Frind, "Contaminant Transport in Fractured Porous media: Analytical Solution for a System of Parallel Fractures", Water Resour. Res., 18, 1634-1642, 1982

4 Sudicky, E. A. and E. O. Frind, "Contaminant Transport in Fractured Porous Media: Analytical Solution for a Two-member Decay Chain in a Single Fracture", Water Resour. Res., 20, 1021-1029, 1984

5 Davis, G. B. and C. D. Johnston, "Comment on 'Contaminant Transport in Fractured Porous Media: Analytical Solutions for a System of Parallel Fractures' by E. A. Sudicky and E. O. Frind", Water Resour. Res., 20, 1321-1322, 1984

6 Chambré, P. L., T. H. Pigford, A. Fujita, T. Kanki, A. Kobayashi, H. Lung, D. Ting, Y. Sato and S. J. Zavoshy, "Analytical Performance Models for Geological Repositories", Chapter 5, LBL-14842, 1982

7 Oberhettinger, F., and L. Badii, "Tables of Laplace Transforms", Springer-Verlag, New York, 1973

8 Abramowitz, M., and I. A. Stegun, "Handbook of Mathematical Functions", Dover, New York, 1965

9 Chambré, P. L., "Notes for Mathematics 120," Theorem 6.1.12, Department of Mathematics, University of California, Berkeley, 1984

LAWRENCE BERKELEY LABORATORY
TECHNICAL INFORMATION DEPARTMENT
UNIVERSITY OF CALIFORNIA
BERKELEY, CALIFORNIA 94720